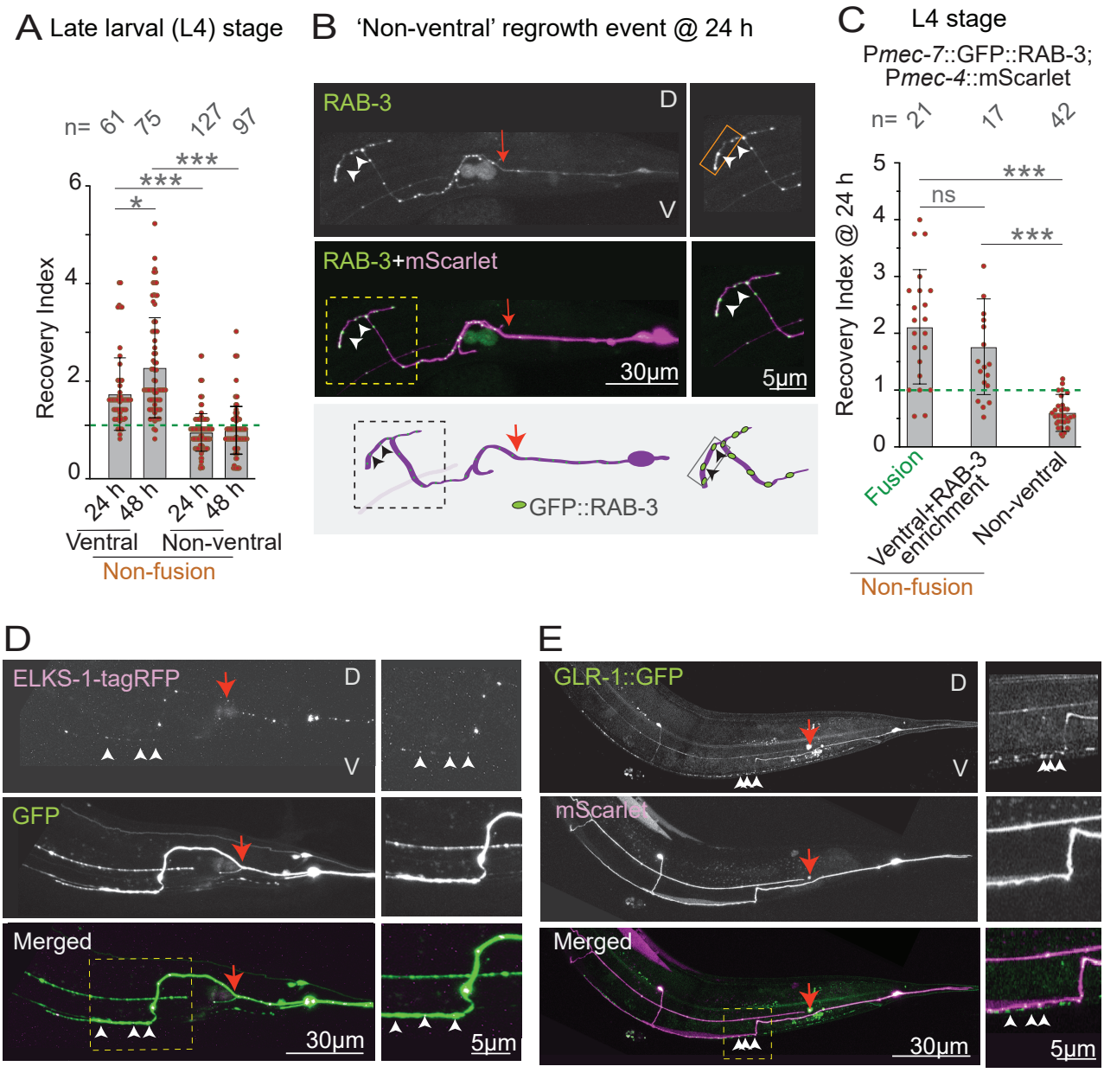

Figure S1: 'Ventral targeting' events often correspond to the enrichment of pre-synaptic reporters at the ventral cord, related to Figure 1.

A) The quantification of the 'Recovery Index' for the 'ventral' and 'non-ventral' regrowth events. N (independent replicates) = 8. B) The confocal image of a 'non-ventral' regrowth event at 24

h postaxotomy of PLM neuron co-expressing the P*mec-7*::GFP::RAB-3 [*jsIs821*] and P*mec-4*::mScarlet [*shrEx209*] reporters. The arrowheads indicate the GFP-RAB-3 punctae localized at the tip of the regrowing axon. The rectangular ROI of 3 µm was used to measure RAB-3 intensity. The red arrow represents the site of injury. C) RI values corresponding to the 'fusion', 'ventral' and 'non-ventral' regrowth events at 24 h postaxotomy in the P*mec-7*::GFP::RAB-3 [*jsIs821*]; P*mec-4*::mScarlet [*shrEx209*] background. N=3-5. D) The confocal image of a 'ventral targeting' event in worm co-expressing P*mec-4*::ELKS-1::tag RFP [*jsIs1075*] and P*mec-7*::GFP [*muIs32*] reporters. The arrowheads indicate the presynaptic enrichment of ELKS-1. E) The confocal image of similar 'ventral targeting' event in worm co-expressing P*rig-3*::GLR-1::GFP [*akIs141*] and *Pmec-4*::mScarlet [*shrEx209*] reporters. The post-synaptic enrichment of GLR-1 is indicated with arrowheads. In A and C, *P < 0.05; ***P < 0.001; ns: non-significant, ANOVA with Tukey's multiple comparisons test. Error bars represent Standard Deviation.

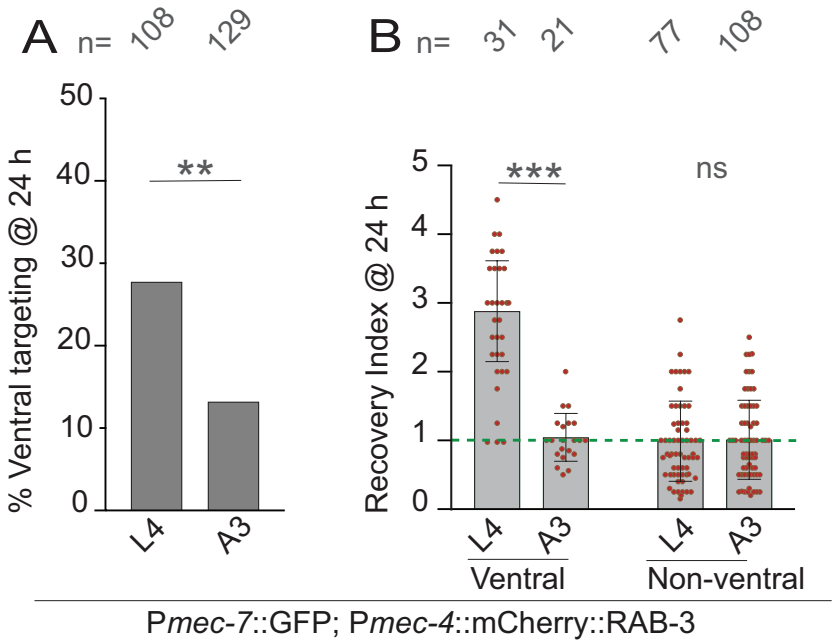

Figure S2: Age related decline in 'ventral targeting' and functional restoration in P*mec-4*:: mCherry::RAB-3 background, related to Figure 2.

A) the percentage of 'ventral targeting' events. B) and RI values corresponding to the different regrowth events in the background expressing P*mec-7*::GFP [*muIs32*] and P*mec-4*::mCherry::RAB-3 [*tbIs227*]. N (independent replicates) = 3-5. In A, **P < 0.01; ns: non-significant; ANOVA with Tukey's multiple comparisons test. In B, ***P < 0.001, Fisher's exact test. Error bars represent Standard Deviation.

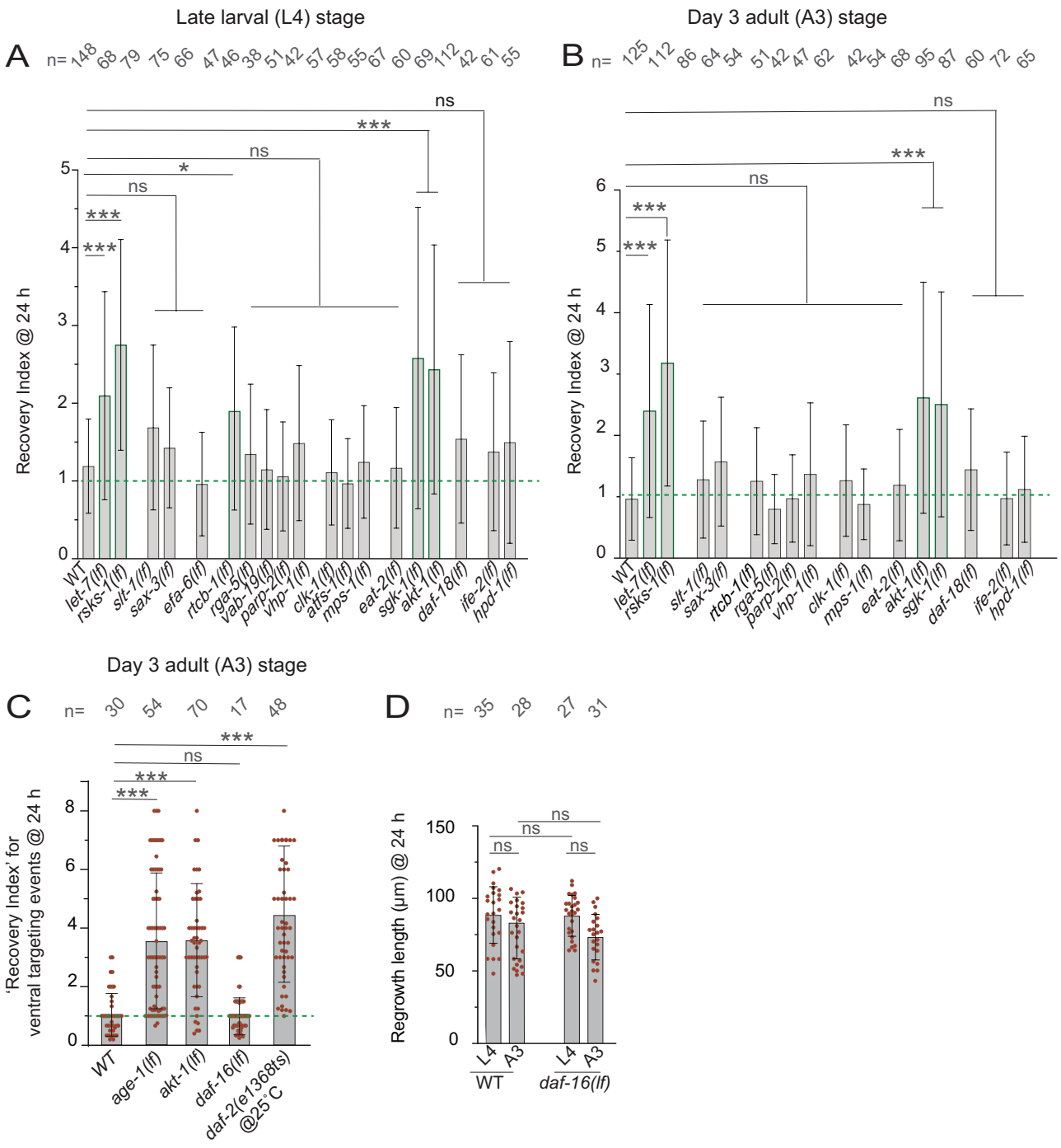

Figure S3: Mutants affecting the Insulin receptor, or the downstream kinases enhances 'ventral targeting' and functional restoration, related to Figure 3.

A-B) The Recovery Index values corresponding to the 'non-fusion' regrowth events in the mutants described in Table S1 at L4 and A3 stages at 24 h postaxotomy**.** N (independent replicates) = 4-8. C) The RI values corresponding to the 'ventral targeting' events in WT and mutants affecting either DAF-2 or downstream kinases at 24 h postaxotomy at A3 stage. N = 5-7. D) The total regrowth length corresponding to the 'non-fusion' events in the WT and *daf-16(lf)* at 24 h postaxotomy. N=3-5. In all plots, *P < 0.05; ***P < 0.001; ns: non-significant; ANOVA with Tukey's multiple comparisons test. Error bars represent Standard Deviation.

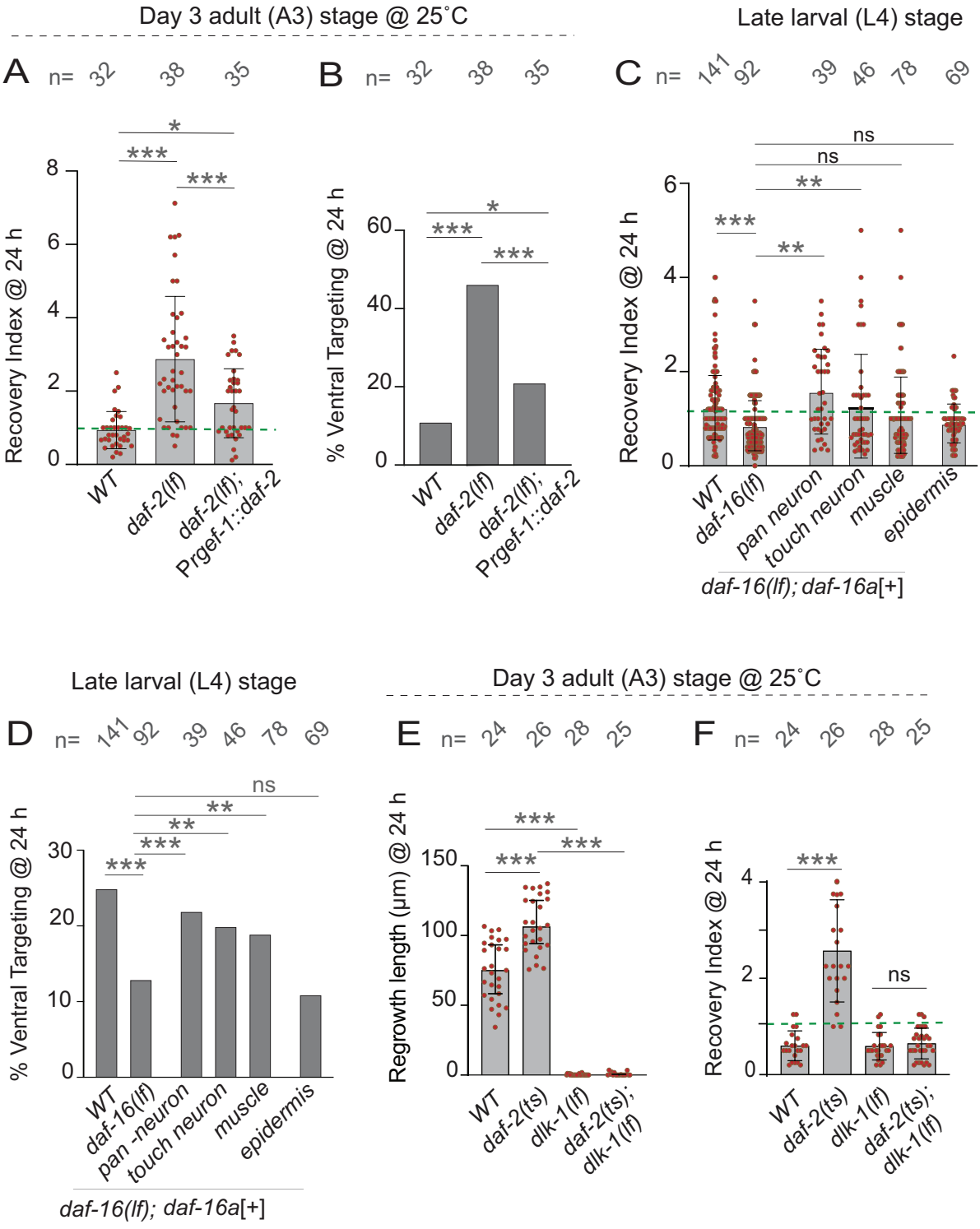

Figure S4: DAF-16 is required both in neuron and muscle for ventral guidance of injured PLM axon, related to Figure 4.

A-B) The quantification of Recovery Index (RI) values (A) and the (%) 'ventral targeting' events (B) corresponding to 'non-fusion' category in WT, *daf-2(m596)* and *daf-2(m596)*; P*rgef-1*::*daf-2* [*hpEx2906*] at 24 h postaxotomy at A3 stage. N (independent replicates) = 3-5. C-D) The RI values (C) and the (%) 'ventral targeting' events (D) corresponding to 'non-fusion' regrowth events in WT, *daf-16(lf)* background with or without the transgene of *daf-16a* expressed under the pan neuronal promoter P*rgef-1* [*shrEx317*], touch neuron-specific promoter P*mec-4* [*shrEx224*], muscle-specific promoter P*myo-3* [*shrEx311*], and the epidermal promoter P*dpy-7* [*shrEx315*]. For both C and D, N=3-5. E-F) The plots show the regrowth length (E) and RI values (F) corresponding to the 'non-fusion' regrowth events at 24 h postaxotomy in WT, *daf-2(e1368ts)*, *dlk-1(lf)* and *daf-2(e1368ts); dlk-1(lf)* backgrounds at A3 stage at 25°C. For both E and F, N= 3. In B and D, *P < 0.05; **P < 0.01; ***P < 0.001; ns: non-significant, Fisher's exact test. In A, C, E and F, *P < 0.05; **P < 0.01; ***P < 0.001; ns: non-significant; ANOVA with Tukey's multiple comparisons test. Error bars represent Standard Deviation.

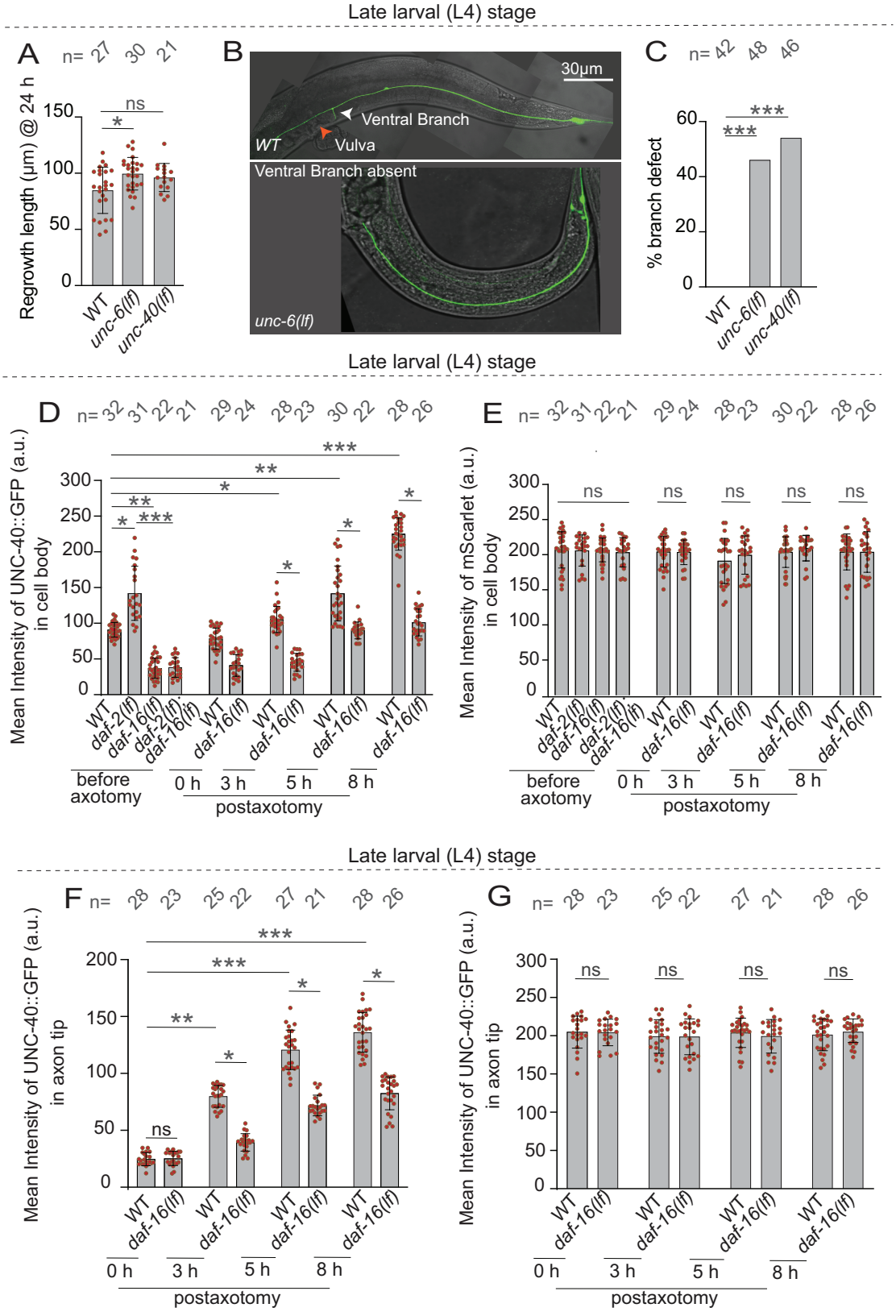

Figure S5: Regulation of the expression and localization of UNC-40 by DAF-16 during axon regeneration, related to Figure 5.

A) The quantification of axon regrowth length corresponding to the 'non-fusion' events in *unc-6(lf)* and *unc-40(lf*) at 24 h postaxotomy at L4 stage. N= 3-4. B) The confocal plus DIC images of PLM neuron expressing P*mec-7*::GFP (*muIs32*) in WT and *unc-6(lf)*. C) The percentage ventral branch defect in *unc-6(lf)* and *unc-40(lf*). N (independent replicates) = 3-5. D-E) The plots represent the mean intensity of *Punc-4*0::UNC-40::GFP [*icIs132*] (D) and P*mec-4*::mScarlet [*shrEx209*] (E) measured from the ROI on the cell body of PLM (in Fig 5D) before and at different time-points after axotomy in WT and *daf-16(lf)*. For both D and E, N= 3-6. F-G) The plots show the mean intensity of P*unc-4*0::UNC-40::GFP [*icIs132*] (F) and Pm*ec-4*::mScarlet [*shrEx209*] (G) from ROI on PLM axon (Fig 5E) before and at different time-points after axotomy in WT and *daf-16(lf)*. In C, ***P < 0.001, Fisher's exact test. In A, D-G, *P < 0.05; **P < 0.01; ***P < 0.001; ns: non-significant; ANOVA with Tukey's multiple comparisons test. Error bars represent Standard Deviation.

Table S1: List of mutants studied for functional restoration assay (excel file).

Click here to download Table S1

Table S2: *Caenorhabditis elegans* strains used in this study.

Click here to download Table S2

Table S3: Strains carrying newly generated extrachromosomal transgenes.

Strains	Transgene	DNA construct	Genetic Background	Concentration,
NBR568	*shrEx209*	P*mec-4*::mScarlet (PNBRGWY54)	N2	5 ng/µl
NBR925	*shrEx435*	P*mec-4*::*unc-9*::GFP (PNBRGWY561)+P*mec-4*::mScarlet (PNBRGWY54)	N2	PNBRGWY561-10ng/ µl PNBRGWY54-5ng/ µl
NBR594	*shrEx224*	P*mec-4*::*daf-16a* (PNBRGWY107)	*daf-16(mu86)* I; *muIs32* (P*mec-7*::GFP) II	10 ng/µl
NBR730	*shrEx311*	P*myo-3*::*daf-16a* (PNBRGWY108)		10 ng/µl
NBR737	*shrEx315*	P*dpy-7*::*daf-16a* (PNBRGWY109)		10 ng/µl
NBR739	*shrEx317*	P*rgef-1*::*daf-16a* (PNBRGWY110)		10 ng/µl
NBR657	*shrEx227*	P*mec-4*::*daf-16f* (PNBRGWY111)		10 ng/µl
NBR732	*shrEx313*	P*myo-3*::*daf-16f* (PNBRGWY112)		10 ng/µl
NBR738	*shrEx316*	P*dpy-7*::*daf-16f* (PNBRGWY113)		10 ng/µl
NBR740	*shrEx318*	P*rgef-1*::*daf-16f* (PNBRGWY114)		10 ng/µl
NBR735	*shrEx320*	P*mec-4*::*daf-16f* (PNBRGWY111)+ P*myo-3*::*daf-16f* (PNBRGWY112)		10 ng/µl (each)
NBR592	*shrEx436*	P*mec-4*::*daf-16f* (PNBRGWY111)	*muIs32* (P*mec-7*::GFP) II	10 ng/µl
NBR593	*shrEx437*	P*myo-3*::*daf-16f* (PNBRGWY112)		10 ng/µl
NBR777	*shrEx389*	P*mec-4*::*dlk-1* (PNBRGWY13)	*muIs32* (P*mec-7*::GFP)II	0.5 ng/µl
NBR779	*shrEx391*	P*mec-4*::*dlk-1* (PNBRGWY13)	*daf-16(mu86)*I; *muIs32* (P*mec-7*::GFP) II	0.5 ng/µl

Table S4: List of the neuronal target genes of DAF-16 categorized under the Gene Ontology term (GO:0097485) or neuronal projection and guidance (excel file).

Click here to download Table S4